

## Quenching and Partitioning process in Ductile Cast Irons

A.J.S.T. da Silva<sup>1,2</sup>, M.F. de Campos<sup>3</sup>, A.S. Nishikawa<sup>1</sup>, W.L. Guesser<sup>4</sup> and H. Goldenstein<sup>1\*</sup>

<sup>1</sup>Department of Metallurgical and Materials Engineering, Escola Politécnica da USP, São Paulo, Brazil

<sup>2</sup>Tupy Fundições S.A., Mauá, Brazil

<sup>3</sup>Universidade Federal Fluminense, Volta Redonda, Brazil

<sup>4</sup>Center of Technological Sciences, Universidade do Estado de Santa Catarina, Joinville, Brazil

A commercial ductile iron alloy was submitted to Quenching and Partitioning (Q&P) process. Samples were austenitized at 900°C for two hours, quenched at 170°C and held at this temperature for 2 minutes and finally were re-heated in temperatures between 300 and 450°C in time intervals between 2 and 180 minutes. The microstructure evaluation was performed with SEM and X-ray diffraction and mechanical properties were measured using uniaxial tensile tests and Charpy tests. In general, the Q&P process is suitable to achieve large fractions of retained austenite in ductile cast irons. The combination of properties thus obtained is very interesting from the engineering point of view, and if the elongation can be increased will provide an alternative to the austempered ductile irons.

**Keywords:** Quenching & Partitioning, Q&P, ductile iron, solid state transformations, austenite, bainite, ADI.

### Introduction

The production of Austempered Ductile Iron (ADI) takes advantage of the effects of the high Si content on the austenite decomposition in the bainitic range, in order to obtain a carbide-free matrix microstructure (ausferrite), where sheaves of bainitic ferrite laths are separated by films or islands of metastable high carbon retained austenite. In ferrous alloys containing Si (or Al), the carbide precipitation step of the bainite transformation is slowed down or suppressed for a time long enough for the carbon from the transformed regions partition and diffuse into the austenite, leading to (meta)stable austenite at room temperature. Similar phenomena occur in TRIP steels, high Si (or Al) low alloy high strength steels containing ausferrite microstructures and also islands of MA (martensite/austenite) microconstituent. In all those material, longer heat treatments lead to carbide precipitation, causing abrupt loss of elongation and fracture toughness, signaling the existence of a finite “process widow”.

Recent developments in steels containing small fractions of retained austenite introduced a new heat treatment route, namely *Quenching and Partitioning* (Q&P). This heat treatment cycle is an alternative route for obtaining multi-phase steel, in which the volumetric fraction of retained austenite is controlled by carbon partition from supersaturated martensite into austenite, allowing the stabilization of austenite<sup>1</sup>.

The concept of Q&P involves transforming partially the austenite to martensite, by quenching to temperatures between Ms (martensite start temperature) and Mf (martensite final temperature), followed by a thermal partitioning treatment, which allows the carbon to diffuse from the supersaturated martensite to the non-transformed austenite. The increased carbon in the austenite lowers its Ms temperature promoting its stabilization<sup>2</sup>. Fig. 1 shows a schematic of the Q&P process. In order to obtain a volume of carbon stabilized austenite, a certain amount of non-transformed austenite after quenching is necessary and also the suppression of carbide precipitation by the presence of silicon or aluminum alloy additions, for a time period long enough for partition to occur<sup>1</sup>.

Studies conducted by several researchers<sup>4-9</sup> proved to be possible to achieve substantive amounts of retained austenite through Q&P heat treatments in silicon containing steels. In these studies it was possible to see the dependence between the fractions of retained austenite (as well as its final carbon content) and the heat treatment conditions. These studies demonstrate that with increased partitioning temperature, the kinetic of the reactions is accelerated, obtaining higher fractions of retained austenite in a shorter period of time. From one point on, this austenite fraction starts decreasing, indicating the beginning of transformation to other type of products (carbide containing phases). Transmission electron microscopy dark field images confirmed that the final structure is composed of thin flakes of austenite between martensite platelets. Furthermore, they evidenced that the Q&P heat treatment cycle is a feasible route for the achievement of combinations of high tensile strength with reasonable tenacity or toughness, using relatively simple Si containing commercial steels. The carbide suppression improves the toughness of steels while the retained austenite will protect the bainitic or martensitic ferrite from the detrimental effects in mechanical properties caused by carbide dispersion.

At the early stage of the development of Q&P, Speers recognized the potential for Q&P ductile cast iron, due to the usual high level of Si found in those alloys, and made preliminary experiments<sup>1</sup>. Undergraduate students at Colorado School of

---

\* Corresponding author, email: hgoldens@usp.br

Mines conducted the work in 2004, with a commercial 3.7%wt C, 2.5%wt Si, 0.34%wt Mn, 0.17%wt Cu ductile cast iron. A limited number of Q&P parameters were assessed in this work, while austenitizing temperature and partitioning time were held constant. The results showed that substantial fractions of carbon-enriched austenite could be retained via Q&P processing, although the austenite levels were found to be lower than obtained via austempering under the processing conditions evaluated. The strengths were greater in the Q&P condition, while the ductility and room temperature impact properties were lower. Speers' group did not pursue this work, though.

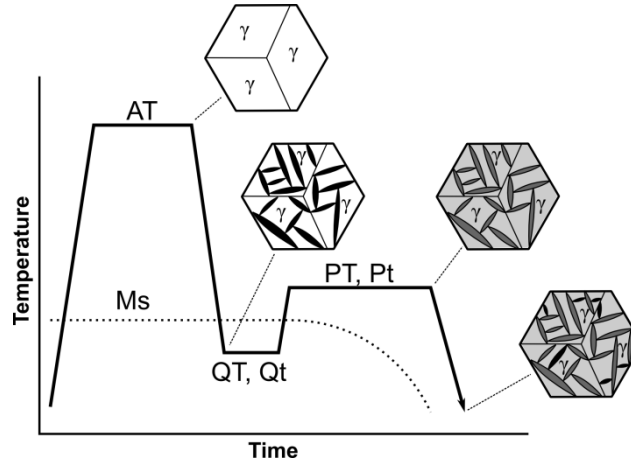


**Fig.1:** Schematic of the Q&P process for production of austenite-containing microstructures. Adapted from Matlock et al<sup>3</sup>.

The main objective of this work is to obtain further knowledge about the behavior of nodular cast irons heat treated in a Q&P cycle. We expected to understand the evolution of the microstructure during the heat treatment in order to identify the existence of a process window, which can be used to obtain improved mechanical properties. The major contribution expected by applying this route in ductile iron is the development of a class of heat-treated nodular cast iron, which can be a technological alternative in applications where the austempered ductile iron are consolidated materials.

## Experimental Procedure

A commercial ductile iron alloy, used in components for the automotive industry, was cast as Y-blocks, following the Brazilian standard NBR 6916. Composition, presented at table 1, is not the optimum composition for ADI, as the Mn level is too high. Nodule counting was 163 nodules/mm<sup>2</sup>, also not very high; a higher nodule count would be beneficial to alleviate the effects of the heterogeneity of the microstructure due to the segregation of chemical elements during solidification.

**Table 1:** Chemical composition of alloys studies in the present work.

| Element            | C    | Si   | Mn   | P    | S    | Cr   | Cu   | Mg   | Ni   |
|--------------------|------|------|------|------|------|------|------|------|------|
| Composition (wt %) | 3.48 | 2.89 | 0.52 | 0.06 | 0.01 | 0.03 | 0.50 | 0.05 | 0.01 |

The Y-blocks were cut into pieces of 25mm thickness, 40mm width and 135mm length and processed under Q&P thermal cycle as described in the Fig. 1. The heat treatment consisted of austenitizing of the specimens at 900°C during 2 hours in a air muffle furnace, quenching into oil bath preheated at the temperature (QT) of 170°C, and reheating until partitioning temperatures (PT) of 300, 375 and 450 °C during various times in the range of 5-180min. The partitioning step was also performed in an air muffle furnace.

The austenitizing temperature was chosen on basis of the parameters typically used in the heat treatment of ADI. In this step carbon redistribute between austenite and graphite, approaching equilibrium levels, although substitutional alloying elements may still remain far from equilibrium compositions. Austenite composition at austenitizing temperature was calculated using computational thermodynamics calculations with Thermo-Calc® software and it is given in table 2. Minor impurities on chemical composition (P, S, and Mg) were not considered in this calculation. This result was coupled with Andrews empirical equation<sup>10,11</sup> (equation 1) and the Ms temperature was estimated as 189°C. Using Koistinen-Marburger<sup>12</sup> relationship (equation 2), the amount of athermal martensite formed at QT from austenite was estimated to be 35 %vol.

$$M_s (\text{°C}) = 539 - 423\%wtC - 30.4\%wtMn - 12.1\%wtCr - 7.5\%wtMo - 7.5\%wtSi \quad (1)$$

$$f_w = 1 - \exp\{-1.1 \cdot 10^{-2} (M_s - QT)\} \quad (2)$$

**Table 2:** Equilibrium austenite chemical composition at 900°C calculated using Thermo-Calc®.

| Element            | C    | Si   | Mn   | Cr   | Cu   | Ni   |
|--------------------|------|------|------|------|------|------|
| Composition (wt %) | 0.71 | 2.97 | 0.52 | 0.03 | 0.51 | 0.01 |

Samples were prepared using conventional metallographic techniques by mechanical polishing and chemical etching using 2% Nital reagent. Scanning electron microscopy (SEM) evaluations were performed using SEM Phillips model XL30 operating at 20kV. X-ray diffraction (XRD) analyses were performed using a Shimadzu model 6000 diffractometer with Co K $\alpha$  radiation. Bragg-Brentano geometry was used and the scanning was made over the interval of  $2\theta = 30-110^\circ$  at steps of  $0.02^\circ$  and 6 sec per step. Retained austenite volume fractions and carbon content were estimated by analysis of diffraction data *via* the Rietveld method using the software TOPAS ACADEMIC 4.1. The amount of carbon dissolved in austenite was obtained using the method developed by Dyson and Holmes<sup>13</sup> through an empirical equation (equation 3) which considers the volumetric changes of crystalline structure with the percentage of alloying elements in solid solution using the change in lattice parameter.

$$a_\gamma = 3.5780 + 0.033\%atC + 0.00095\%atMn + 0.002\%atNi + 0.0006\%atCr + 0.0031\%atMo + 0.0018\%atV \quad (3)$$

Mechanical evaluation was carried out by impact Charpy tests from samples machined from heat treated blocks. Impact tests were carried out in a 30 KPM Wolpert machine, model PW 20/30K according to NBR 6157 standard. Tensile tests samples were also machined from heat treated blocks. Uniaxial tensile strength tests were conducted in an EMIC universal machine model DL 20000 at a loading speed of 1 mm/min.

## Results

### Analyses of microstructures

The analysis of the microstructure *via* SEM method showed that the microstructure of almost all treated samples presents pronounced differences between the intercellular zones and the areas around graphite nodules, as can be seen in Fig. 2. In the areas surrounding the nodules, it was observed the presence of partitioned martensite (i.e., martensite formed during quenching step and tempered during partitioning step) and ausferrite (bainitic ferrite + retained austenite). On the other hand, the intercellular areas were composed predominantly by fresh martensite, probably formed by the transformation of unstable austenite during final cooling. Due to segregation, the intercellular area presented lower  $M_s$  value and thus remained austenitic during quenching step. In the absence of athermal martensite, the only way to carbon-enrich austenite in these areas would be the formation of ausferrite. In shorter partitioning times there was not enough time for substantial formation of ausferrite and, consequently, during the final cooling the unstable austenite transformed into martensite. For longer partitioning times the intercellular austenite fully decomposes into ausferrite, as can be seen in Fig. 3.

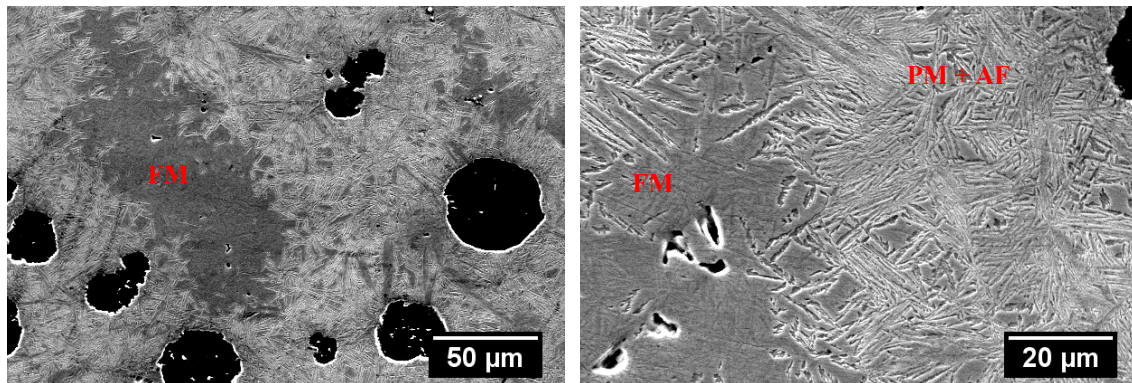


**Fig.2:** Microstructure of the sample partitioned at 300°C during 2 minutes, showing the differences of microstructures around the nodules (PM = partitioned martensite, AF = ausferrite) and around the eutectic cells (FM = fresh martensite).



Chemical elements such as manganese, molybdenum and chromium segregate towards eutectic cell boundaries. In practice, areas around the nodules and intercellular areas behave almost as two different alloys, with different compositions. Therefore, the kinetic of transformations resulting from heat treatment will differ on both areas<sup>14</sup>. This phenomenon will possibly allow that, in the same heat treatment, austenite will be stabilized by carbon in areas close to the graphite nodules whereas in the intercellular areas there is still austenite with low carbon content, which will transform to fresh martensite during final cooling. It's known that differences in substitutional elements chemical composition will not relax on the relatively short austenitizing times applied in this study. Thus different percentages of carbon and substitutional elements will be present, either in equilibrium with graphite or in intercellular areas and around the nodule at the end of the austenitizing process. As a consequence the Ms temperature and the amount of martensite (either the real values and those predicted by equations 1 and 2) will be different in these areas.

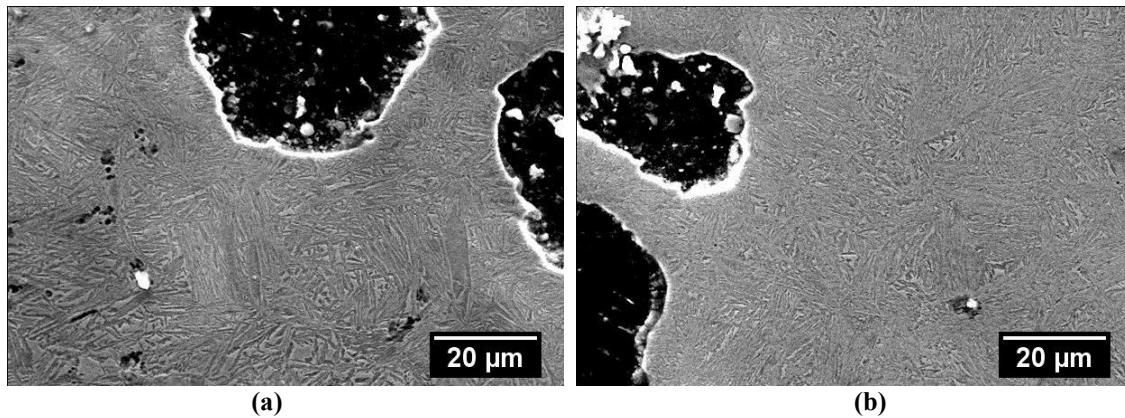


**Fig.3:** Sample partitioned at 300 °C during (a) 60 minutes and (b) 120 minutes. It's possible to observe that intercellular areas were fully transformed into ausferrite.

SEM micrographs presented in Fig. 4 show the matrix microstructure near a graphite nodule. As pointed earlier, it's possible to distinguish ausferrite (thin needle-like product) from partitioned martensite (PM) that was formed during first quenching and whose carbon was partitioned during the isothermal heat treatment. The carbon of the plate martensite observed around the nodule diffused to the remaining austenite, eliminating martensite supersaturation. In this way, this product is plate martensite (morphologically) but with low carbon content and body centered cubic structure, similar to ferrite. It's worth noting that the amount of partitioned martensite seems to be lower than the predicted amount estimated by Koistinen-Marburger (KM) equation. There are two possible explanations to this observation: KM equation adjusting coefficients are sensitive to alloy chemical composition and thus may introduce an error to the estimative. Moreover, the sample holding time at quenching temperature may not have been long enough to allow the thermal stabilization between the sample and the oil bath, leading to a lower amount of martensite.

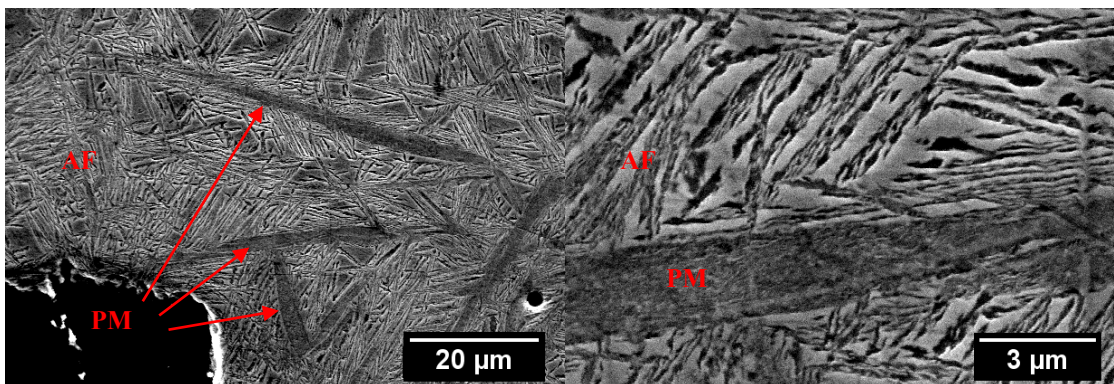


**Fig.4:** Sample partitioned at 300 °C during 5 minutes, showing ausferritic structure (AF) as well depleted carbon martensitic areas formed during quenching (PM).

The two martensitic areas presented in Fig. 2 and Fig. 4 have distinct morphology and mechanical properties due to different carbon contents in solution. The low carbon content of the martensite present around graphite nodules allows this

phase to present lower hardness. On the other hand, martensite in the intercellular areas has higher carbon content; therefore, this phase is potentially brittle due to its high hardness, tetragonality and level of residual stresses.

Summarizing, the final microstructure obtained through quenching and partitioning in ductile cast irons is composed of graphite nodules formed during solidification and a mixture of ausferrite (bainitic ferrite free of carbides and retained austenite) with high and low carbon (carbon depleted) martensite.

### Analyses of XRD results

X-ray diffraction tests were carried out with the purpose of measuring the fractions of retained austenite in the samples. The charts in Fig. 5 show that it is possible to obtain sizeable fractions of retained austenite with considerable carbon content dissolved in it, depending on the partitioning conditions. The transformation kinetics during the partitioning step shows strong dependence on temperature. In general, the kinetics is accelerated at higher partitioning temperatures. Samples partitioned at 300°C presented retained austenite fractions with increasing tendency during the 180 minutes of the partitioning cycle, while the samples partitioned at 450°C shows the retained austenite peaking in the first minutes of the partitioning cycle followed by fast subsequent decreasing contents, indicating a minimal or nonexistent process window for this temperature.

Fig. 5b shows that higher austenite carbon content was obtained faster when higher partitioning temperatures were used. In all conditions, carbon content increases during the initials heat treatment times. After certain time, it is noticed that the carbon content dissolved in austenite decreases. This behavior is evidence that after certain time intervals the austenite decomposes into other types of products, probably carbides of the second stage of bainitic reaction, the same phenomenon that occurs in ductile cast iron subjected to long austempering times.

It also can be noted that for the sample partitioned at 300 °C in the shortest time (2 min) austenite carbon content calculated from the lattice parameter is smaller than the expected austenite initial composition. This might be due to the fact that at this partitioning time austenite is not sufficiently carbon-enriched to stabilize itself. Hence, fresh martensite may have formed at the final cooling, exerting compressive stresses on the austenite surrounding regions, thus explaining the smaller lattice parameter observed. Similar results were reported by Golovchiner<sup>15</sup> in Fe-Ni alloys, and Toji et al<sup>16</sup> for a Q&P steel.

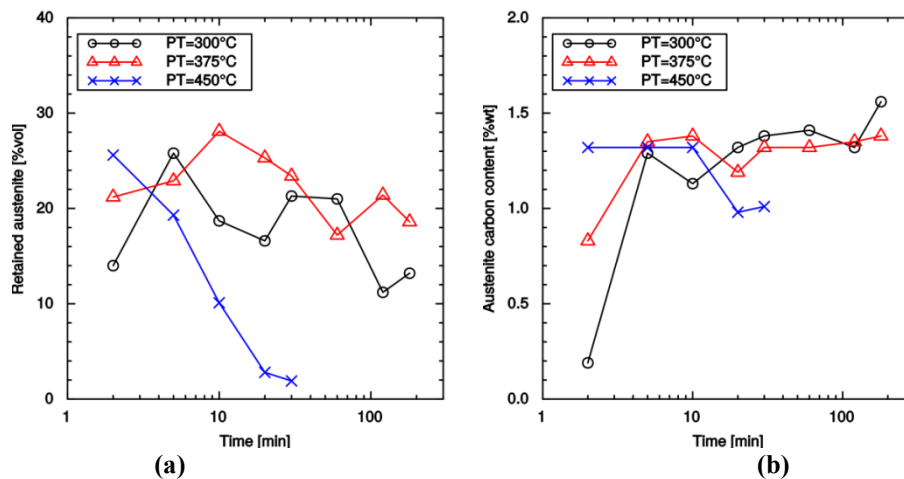


**Fig.5:** (a) Retained austenite fractions obtained in all partitioning conditions. (b) Carbon content in solid solution in retained austenite obtained in all partitioning conditions.

### Mechanical properties

Impact tests were performed to provide an estimate of the toughness of this new class of material. The data presented in Fig. 6 shows that the impact energy initially increases and after some time of partitioning treatment starts to decrease, characterizing a process window. For 300°C the energy decreases after 120 min, for 375°C after 20 minutes and for 450°C after only 10 minutes. The initial increase is explained by the presence of stabilized retained austenite, confirmed by X-ray diffraction. The maximum impact energy results obtained were 87.2 J on samples partitioned at 300°C for 120 minutes, 92.2 J on samples partitioned at 375°C for 20 minutes and 58.8 J on samples partitioned at 450°C for 5 minutes. A time interval that produces optimized properties can be observed for each heat treatment properties used in this study. If the heat treatment time is longer or shorter than the process window, the mechanical properties will be decreased.

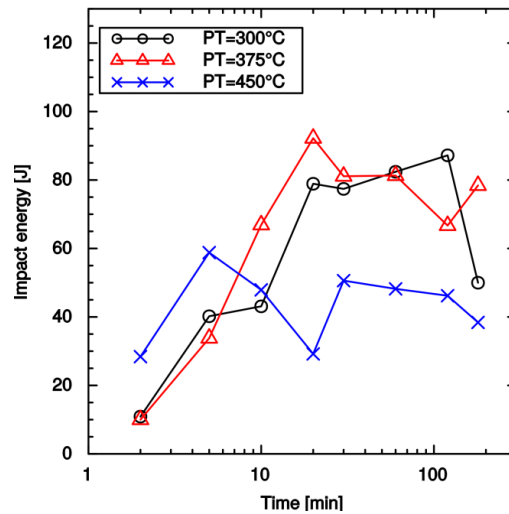


**Fig. 6:** Impact energy (Joules) of all heat treatment conditions.

Analyzing Fig. 7 it is possible to observe that both Ultimate Tensile Strength (UTS) and Yield Strength (YS) presents a tendency to increase during the partitioning heat treatment. This result is in agreement with the kinetic of ausferrite formation in the intercellular areas. For all tested conditions, the higher values of tensile/yield strength were observed after longer partitioning times. In the sample partitioned at 300 °C, there was a large increase of the mechanical properties only after 60 minutes of treatment, presumably because of the slow kinetics of ausferrite formation at this temperature. After 120 min, the impact energy and total elongations started to fall even for the 300° C treatment.

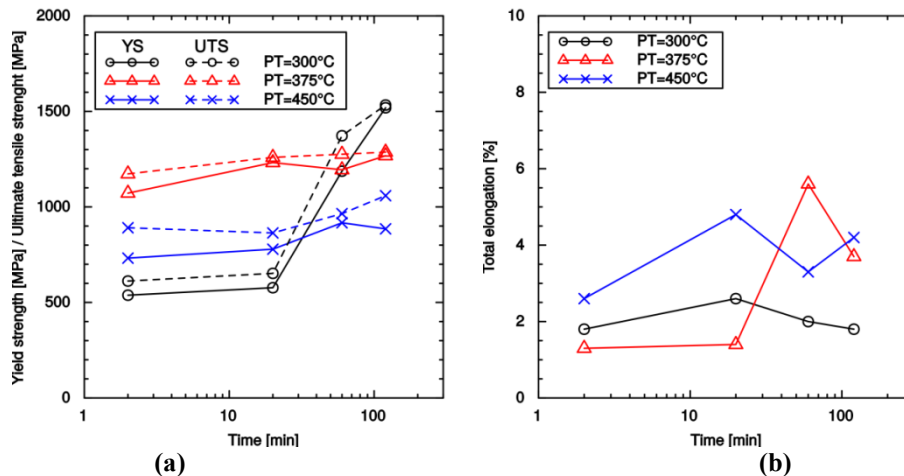


**Fig. 7:** Tensile properties of all conditions tested. (a) Yield strength (YS) and ultimate tensile strength (UTS). (b) Total elongation.

## Discussion

The concept of process window is widely used on the austempered ductile irons and consists of the time intervals and temperatures in which it is possible to obtain optimal mechanical properties<sup>14</sup>. If the holding time at the austempering temperature is too short, it is possible that certain portion of austenite will not be enriched enough by carbon to be able to reach thermal stability and will transform to fresh martensite during cooling to room temperature, decreasing the material toughness (decrease on elongation and impact energy). On the other hand, if the time is too high, the second stage of bainitic reaction will be reached, in which the austenite, supersaturated in carbon, will decompose precipitating carbides. This phenomenon will also decrease the toughness of material. In this way, for each austempering temperature used in heat treatment, it exists a time interval where the material present optimal properties. In general, higher austempering temperatures will produce more tight process windows, because the transformations during heat treatment will be accelerated<sup>14</sup>.

Fig. 8 presents a comparison between the mechanical properties of the samples used in this study with the mechanical properties of austempered ductile iron presented in ASTM A897 standard<sup>17</sup>. It is possible to see that the Q&P heat treatments were not able to obtain the elongations specified for austempered ductile irons (ADI), with the exception of one sample treated at 375°C for 60 minutes.

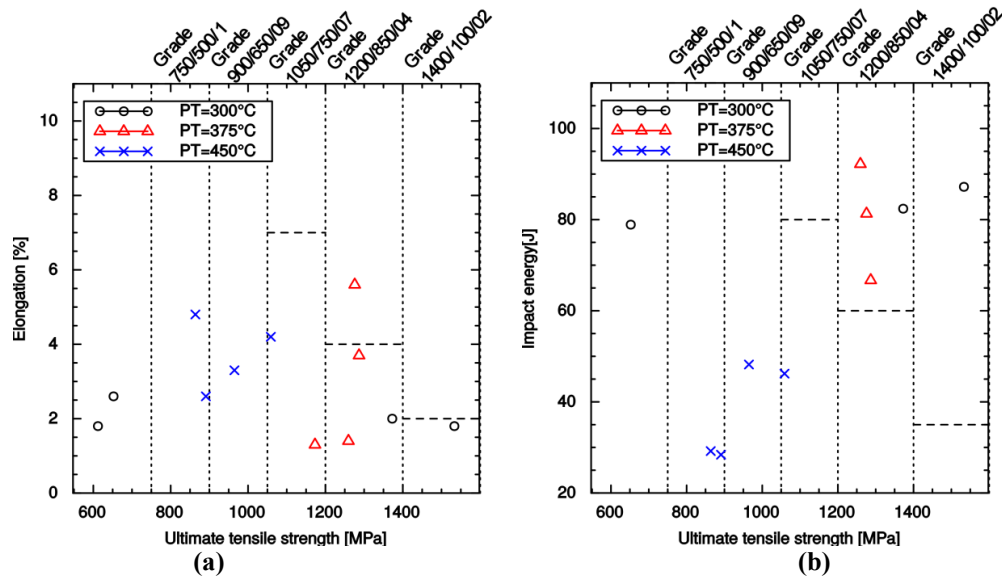


**Fig. 7:** Mechanical properties map comparing ADI with quenching and partitioning ductile cast iron. Dashed lines represent ASTM A897 specifications.

A possible explanation for this failure is suggested by the difference in microstructure between the regions near the nodules and the intercellular regions, an indication of chemical heterogeneity between the two regions, due to segregation during the solidification. As discussed earlier, the segregation of chemical elements will change the local kinetics of transformation mainly at intercellular areas, richer in elements such as manganese and molybdenum that segregate to the last region to solidify. In the specific case of the alloy used in this study, the formation of fresh martensite during the final cooling in the segregated intercellular areas was due to two main effects: the  $M_s$  temperature of the intercellular areas is reduced below the quenching temperature, blocking the formation of martensite during the first step of heat treatment; secondly, the formation of ausferrite in the intercellular areas will be difficult, producing large areas of cell boundary containing non-stabilized austenite, which will be transformed into martensite in the final cooling. Thus, high manganese contents shortens the process window, making less probable the stabilization of the intercellular austenite for smaller partitioning times. At the same time, the end of the process window is accelerated near the nodules, for the same reasons. This difference causes the process window of one region to have a minimal overlap with the process window of the other; one region starts to precipitate carbides before the other has stabilized the austenite, in the same sample. This is probably what happened at 450°C causing the low elongation and fracture energy obtained for partitioning at this temperature. Using as initial material a cast iron with a higher nodule count through advanced inoculation techniques and lowering the Mn content could help minimize intercellular segregation, thus improving significantly the elongation.

The application of Q&P to thicker parts will eventually require the use of alloying elements (Mo, Mn) in order to increase hardenability and therefore the effect of segregation of these elements tends to be potentiated. In addition to their effects on the kinetics of isothermal transformations, both manganese and molybdenum tend to form eutectic carbides at the end of the solidification, which are difficult to dissolve during the austenitizing step. These carbides will act as nucleation sites for cracks, harming the mechanical properties. An option is to use nickel and copper additions, as these alloying elements do not tend to segregate in intercellular areas. Another way to minimize the segregation effect is to increase the amount of eutectic cells through inoculation. An effective inoculation can significantly increase the number of eutectic cells in the ductile cast irons and consequently improve the distribution of segregation in the microstructure<sup>14</sup>.

The precipitation of carbides can occur owing to the use of too long times or too high temperatures during isothermal treatment. The experimental data of volumetric fraction of retained austenite and carbon content in the austenite that were presented in this study shows that higher partitioning temperatures will accelerate the kinetics of reaction causing higher percentages of retained austenite and carbon content in solution for shorter times. This provides evidence that higher temperatures accelerate the partition of carbon into the austenite, and also the precipitation of other products, such as ausferrite or carbides from second stage of bainitic reaction, the last one with embrittlement effect. In this way, the correct



# 10<sup>th</sup> International Symposium on the Science and Processing of Cast Iron – SPCI10

selection of partitioning temperature is the key to obtain the best combination of mechanical properties. The silicon content also has a role, preventing carbide formation in austempered ductile irons. So the correct selection of the silicon content added to the base alloy is an important way to optimize the process window and therefore the mechanical properties.

## Conclusions

1. Q&P is a viable route to obtain ductile irons with considerable volumetric fractions of retained austenite.
2. The microstructural analysis showed that the microstructure resulting from quenching and partition heat treatments of a conventional ductile iron is composed of a mixture of partitioned martensite (low carbon) + fresh martensite + ausferrite (bainitic ferrite free of carbides + retained austenite).
3. In intercellular areas, fresh martensite formed from unstable austenite is predominant. In other areas, the presence of ausferrite formed in the partitioning cycle will predominate. These differences are originated from the gradient of chemical composition between these areas.
4. The process window concept can be applied to ductile cast irons heat treated with a Q&P cycle. The heterogeneities between the intercellular region and the neighborhood of the nodules cause a difference on the kinetics, which can
5. The combination of properties thus obtained is very interesting from the engineering point of view, and if the elongation can be increased will provide an alternative to the austempered ductile irons in applications in which the latter has already been consolidated.

## References

1. J.G. Speer, D.V. Edmonds, F.C. Rizzo F.C. and D.K. Matlock: *Curr. Opin. Solid State Mater. Sci.*, 2004, 8, 219-237.
2. G.A. Thomas, J.G. Speer and D.K. Matlock: *Iron Steel Technol.*, 2008, 10, 209-217.
3. D.K. Matlock, V.E. Bräutigam and J.G. Speer: *Mater. Sci. Forum*, 2003, 426-432, 1089-1094.
4. A.M. Streicher, J.G. Speer, D.K. Matlock and B.V. Edmonds: Proc. Int. Conf. on 'Advanced High Strength Sheet Steels for Auto Applications', Warrendale, USA, 2004, 51-62.
5. D.V. Edmonds, K. He, F.C. Rizzo, B.C. De Cooman, D.K. Matlock and J.G. Speer: *Mater. Sci. Eng. A*, 2006, 438-440, 25-34.
6. N. Zhong, X. Wang, Y. Rong and L. Wang: *J. Mater. Sci.*, 2006, 22, 751-754.
7. E. De Moor, S. Lacroix and L. Samek: Proc. 3rd Int. Conf. on 'Advanced Structural Steels', Gyeongju, Korea, August 2006.
8. S.S. Nayak, R. Anumolu, R.D.K. Misra, K.H. Kim and D.L. Lee: *Mater. Sci. Eng. A*, 2008, 498, 442-456.
9. A.J.J. Clarke, J.G. Speer, D.K. Matlock, F.C. Rizzo, D.V. Edmonds and M.J. Santofimia: *Scr. Mater.*, 2009, 61, 149-152.
10. K.W. Andrews: *Iron Steel Inst. J.*, 1965, 203, 721-727.
11. I.A. Yakubtsov and G.R. Purdy: *Metall. Mater. Trans. A*, 2011, 43, 437-446.
12. D.P. Koistinen and R.E. Marburger: *Acta Metall.*, 1959, 7, 59-60.
13. D. Dyson and B. Holmes: *J. Iron Steel Inst.*, 1970, 208, 469-470.
14. W.L. Guesser: in 'Propriedades Mecânicas dos Ferros Fundidos'; 2009, São Paulo, Edgar Blücher Ltda.
15. K.Y. Golovchiner: *Phys. Met. Metallogr.*, 1974, 37, 126-130.
16. Y. Toji, H. Matsuda, M. Herbig, P.P. Choi and D. Raabe: *Acta Mater.*, 2014, 65, 215-228.
17. ASTM International: 'ASTM A897/A897M-06 - Standard Specification for Austempered Ductile Iron Castings', 2011.

## Acknowledgement

The authors acknowledge the support of CAPES – Coordenação de Aperfeiçoamento de Pessoal de Nível Superior and CNPq – Conselho Nacional de Desenvolvimento Científico e Tecnológico through grants for some of the authors. The authors thanks Tupy Fundições S.A., Mauá, Brazil for providing the cast iron samples and access to facilities.